Inorg. Chem. **2008**, *47*, 4392−4400

Synthesis and Characterization of (3,1) $Ru_2(F_3ap)_4(NCS)$ and (3,1) $Ru_2(F_3ap)_3(F_2Oap)(NCS)$ Where F_3ap Is the 2-(2,4,6-Trifluoroanilino)pyridinate Anion

Minh Nguyen,[†] Tuan Phan,[†,‡] Eric Van Caemelbecke,[†,§] Xin Wei,[‡] John L. Bear,[*,†] and Karl M. Kadish[*,†]

Department of Chemistry, University of Houston, Houston, Texas 77204-5003, Department of Chemistry, Texas Southern University, Houston, Texas 77004, and Houston Baptist University, 7502 Fondren Road, Houston, Texas 77074-3298

Received January 16, 2008

Two isothiocyanate diruthenium complexes, (3,1) $Ru_2(F_3ap)_4(NCS)$ **1** and (3,1) $Ru_2(F_3ap)_3(F_2Oap)(NCS)$ **2** (where F_3ap = 2,4,6-trifluoroanilinopyridinate anion), were synthesized from (3,1) $Ru_2(F_3ap)_4Cl$ and SCN^- under different experimental conditions. Each compound was examined as to its structural, electrochemical, spectroscopic, and magnetic properties. Compound **1** contains three unpaired electrons as its parent compound but **2** is diamagnetic. The X-ray molecular structures of **1** and **2** reveal that the NCS group is coordinated to the dimetal unit via nitrogen in both compounds with the Ru−N−C bond angle being 176.5° for **1** and 166.0° for **2**. An elongation of the Ru−Ru bond distance and a shortening of both the $Ru-N_p$ (p = pyridyl) and the $Ru-N_a$ (a = anilino) bond lengths is seen upon going from (3,1) $Ru_2(F_3ap)_4Cl$ to **2**, but the conversion of (3,1) $Ru_2(F_3ap)_4Cl$ to **1** does not affect significantly structural features of the $Ru_2(L)_4$ framework. Compound **1** undergoes one reduction and two oxidations, all three of which involve the dimetal core, whereas **2** undergoes two metal-centered reductions, one metal-centered oxidation, and one ligand-based oxidation due to the presence of the F_2Oap ligand on the Ru_2 complex. The reactivity of **1** with SCN^- was also investigated.

Introduction

Diruthenium complexes supported by *N*,*N*′-bidentate ligands are known to exhibit rich redox properties and can exist in a number of different dimetal oxidation states ranging from Ru_2^{3+} to Ru_2^{7+} depending upon the specific axial and bridging ligands.[1–34] Several laboratories have reported that these types of dimetal complexes can be used as building blocks for linear arrays or 2D networks through axial or equatorial coordination of ditopic and tetrapic

* To whom correspondence should be addressed. E-mail: kkadish@uh.edu.
† University of Houston.
‡ Texas Southern University.
§ Houston Baptist University.

(1) Bear, J. L.; Li, Y.; Han, B.; Van Caemelbecke, E.; Kadish, K. M. *Inorg. Chem.* **2001**, *40*, 182–186.
(2) Bear, J. L.; Li, Y.; Cui, J.; Han, B.; Van Caemelbecke, E.; Phan, T.; Kadish, K. M. *Inorg. Chem.* **2000**, *39*, 857–861.
(3) Bear, J. L.; Li, Y.; Han, B.; Van Caemelbecke, E.; Kadish, K. M. *Inorg. Chem.* **1997**, *36*, 5449–5456.
(4) Bear, J. L.; Han, B.; Huang, S.; Kadish, K. M. *Inorg. Chem.* **1996**, *35*, 3012–21.
(5) Bear, J. L.; Chen, W.-Z.; Han, B.; Huang, S.; Wang, L.-L.; Thuriere, A.; Van Caemelbecke, E.; Kadish, K. M.; Ren, T. *Inorg. Chem.* **2003**, *42*, 6230–6240.
(6) Bear, J. L.; Han, B.; Huang, S. *J. Am. Chem. Soc.* **1993**, *115*, 1175–7.
(7) Campos-Fernandez, C. S.; Thomson, L. M.; Galan-Mascaros, J. R.; Xiang, O.; Dunbar, K. R. *Inorg. Chem.* **2002**, *41*, 1523–1533.
(8) Chen, W.-Z.; Ren, T. *Organometallics* **2005**, *24*, 2660–2669.
(9) Chen, W.-Z.; Ren, T. *Inorg. Chem.* **2003**, *42*, 8847–8852.
(10) Cotton, F. A.; Stiriba, S.-E.; Yokochi, A. *J. Organomet. Chem.* **2000**, *595*, 300–302.
(11) Cotton, F. A.; Torralba, R. C. *Inorg. Chem.* **1991**, *30*, 2196–2207.
(12) Kuehn, F. E.; Zuo, J.-L.; Fabrizi de Biani, F.; Santos, A. M.; Zhang, Y.; Zhao, J.; Sandulache, A.; Herdtweck, E. *New J. Chem.* **2004**, *28*, 43–51.
(13) Li, Y.; Han, B.; Kadish, K. M.; Bear, J. L. *Inorg. Chem.* **1993**, *32*, 4175–4176.
(14) Kadish, K. M.; Phan, T. D.; Wang, L.-L.; Giribabu, L.; Thuriere, A.; Wellhoff, J.; Huang, S.; Van Caemelbecke, E.; Bear, J. L. *Inorg. Chem.* **2004**, *43*, 4825–4832.
(15) Xu, G.; Ren, T. *J. Organomet. Chem.* **2002**, *655*, 239–243.
(16) Kadish, K. M.; Nguyen, M.; Van Caemelbecke, E.; Bear, J. L. *Inorg. Chem.* **2006**, *45*, 5996–6003.
(17) Ren, T.; Parish, D. A.; Xu, G.-L.; Moore, M. H.; Deschamps, J. R.; Ying, J.-W.; Pollack, S. K.; Schull, T. L.; Shashidhar, R. *J. Organomet. Chem.* **2005**, *690*, 4734–4739.

10.1021/ic8000703 CCC: $40.75
Published on Web 04/17/2008

linkers.[14,17,18,20,35–45] One of the ditopic linkers is CN^-, which has been used as an N-donor ligand to diruthenium complexes to form extended arrays[46,47] or molecular complexes.[48]

It was also recently reported that diruthenium complexes obtained by the substitution of Cl^- by SCN^- have structural features that parallel those of the parent chloro complex but have significant differences in magnetic properties.[42,45] However, the effect of SCN^- on the Ru_2 core has been documented to depend on the type of equatorial ligands, which, in turn, might be related to the gap between the π^* and δ^*. For instance, Barral et al.[42,45] showed that there was no change in the spin state configuration of the Ru_2 complexes upon going from the trimer $[Ru_2(DPhF)_3Cl]_3-[C_6H_3\text{-}1,3,5\text{-}(CO_2)_3]$ to $[Ru_2(DPhF)_3(NCS)]_3-[C_6H_3\text{-}1,3,5\text{-}(CO_2)_3]$ (DPhF is the *N*,*N*′-diphenylformamidinate anion) but the Ru_2 complexes $Ru_2(O_2CMe)(DPhF)_3Cl$ and $Ru_2(O_2CMe)(DPhF)_3(NCS)$ differ in their number of unpaired electrons.[42,45] We therefore wished to know whether a similar trend would be seen upon reacting SCN^- with (3,1) $Ru_2(F_3ap)_4Cl$ and especially whether the reactivity of this compound with SCN^- would parallel what has been reported in the case of CN^-.[2,5] This is investigated in the present study, which describes the reaction of (3,1) $Ru_2(F_3ap)_4Cl$ (F_3ap = 2,4,6-trifluoroanilinopyridinate anion) with SCN^- under different solution conditions and also reports the reactivity for one of the resulting isothiocyanato **1** with excess SCN^- anion.

Experimental Section

Chemicals and Reagents. Ultra-high purity nitrogen was purchased from Matheson-Trigas. GR graded dichloromethane, THF, diethyl ether, hexanes, acetones, absolute dichloromethane (for electrochemistry and UV–vis spectroelectrochemistry measurements), and tetra-*n*-butylammonium thiocyanate (TBASCN) were all obtained from EMD, VWR, Fluka, or Aldrich and were used as received. Tetra-*n*-butylammonium perchlorate (TBAP) purchased from Fluka was recrystallized from ethyl alcohol and stored in a vacuum oven at 40 °C for a few weeks prior to use. 2-(2,4,6-trifluoroaniline), ($C_6H_4NF_3$), 2-bromopyridine (C_5H_4BrN), lithium chloride (LiCl), ruthenium chloride hydrate ($RuCl_3 \cdot 3H_2O$), and $CDCl_3$ (99.8% atom in D for NMR measurements) were purchased from Aldrich and used without additional purification. Silica gel (Merck 230–400, mesh 60 Å) was purchased from Sorbent Technologies, Inc. and used as received. The (3,1) isomer of $Ru_2(F_3ap)_4Cl$ was synthesized as described in the literature.[25]

Instrumentation. Cyclic voltammetry was carried out with an EG&G model 263A potentiostat/galvanostat. A three-electrode system was used and consisted of a glassy carbon or platinum-disk working electrode, a platinum-wire auxiliary electrode, and a homemade saturated calomel electrode (SCE) as the reference electrode. The SCE was separated from the bulk of the solution by a fritted-glass bridge of low porosity containing the solvent/supporting electrolyte mixture. All potentials are referenced to the SCE, and measurements were carried out at room temperature. UV–vis spectroelectrochemical experiments were performed with a homemade spectroelectrochemical thin-layer cell[49] and a Hewlett-Packard model 8453 diode array spectrophotometer.

^1H NMR measurements were recorded at room temperature on a General Electric QE-300 Plus spectrometer and were referenced to tetramethylsilane (TMS). Magnetic susceptibilities were measured according to the Evans' method[50] on a General Electric QE-300 FT NMR spectrometer in $CDCl_3$ with TMS as the internal reference compound. IR spectra were measured on a Thermo Nicolet AVATAR 370 Fourier Transform (FT) IR spectrophotometer. Mass spectra were obtained with an Applied Biosystem Voyager DE-STR MALDI-TOF mass spectrometer equipped with a nitrogen laser (337 nm) at the University of Houston Mass Spectrometry Laboratory. Elemental analysis was carried out by Atlantic Microlab Inc.

(18) Ren, T. *Organometallics* **2005**, *24*, 4854–4870.
(19) Kadish, K. M.; Phan, T. D.; Giribabu, L.; Shao, J.; Wang, L.-L.; Thuriere, A.; Van Caemelbecke, E.; Bear, J. L. *Inorg. Chem.* **2004**, *43*, 1012–1020.
(20) Han, B.; Shao, J.; Ou, Z.; Phan, T. D.; Shen, J.; Bear, J. L.; Kadish, K. M. *Inorg. Chem.* **2004**, *43*, 7741–7751.
(21) Cotton, F. A.; Murillo, C. A.; Reibenspies, J. H.; Villagran, D.; Wang, X.; Wilkinson, C. C. *Inorg. Chem.* **2004**, *43*, 8373–8378.
(22) Angaridis, P.; Cotton, F. A.; Murillo, C. A.; Villagran, D.; Wang, X. *Inorg. Chem.* **2004**, *43*, 8290–8300.
(23) Xu, G.-L.; Jablonski, C. G.; Ren, T. *Inorg. Chim. Acta* **2003**, *343*, 387–390.
(24) Xu, G.-L.; Jablonski, C. G.; Ren, T. *J. Organomet. Chem.* **2003**, *683*, 388–397.
(25) Kadish, K. M.; Wang, L.-L.; Thuriere, A.; Van Caemelbecke, E.; Bear, J. L. *Inorg. Chem.* **2003**, *42*, 834–843.
(26) Kadish, K. M.; Wang, L.-L.; Thuriere, A.; Giribabu, L.; Garcia, R.; Van Caemelbecke, E.; Bear, J. L. *Inorg. Chem.* **2003**, *42*, 8309–8319.
(27) Hurst, S. K.; Xu, G.-L.; Ren, T. *Organometallics* **2003**, *22*, 4118–4123.
(28) Xu, G.; Campana, C.; Ren, T. *Inorg. Chem.* **2002**, *41*, 3521–3527.
(29) Bear, J. L.; Wellhoff, J.; Royal, G.; Van Caemelbecke, E.; Eapen, S.; Kadish, K. M. *Inorg. Chem.* **2001**, *40*, 2282–2286.
(30) Lin, C.; Ren, T.; Valente, E. J.; Zubkowski, J. D. *J. Chem. Soc., Dalton Trans.* **1998**, 571–576.
(31) Lin, C.; Ren, T.; Valente, E. J.; Zubkowski, J. D.; Smith, E. T. *Chem. Lett.* **1997**, 753–754.
(32) Bear, J. L.; Li, Y.; Han, B.; Kadish, K. M. *Inorg. Chem.* **1996**, *35*, 1395–8.
(33) Cotton, F. A.; Ren, T. *Inorg. Chem.* **1991**, *30*, 3675–3679.
(34) Goerner, H.; Kuhn, H. J.; Schulte-Frohlinde, D. *EPA Newsletter* **1987**, *31*, 13–19.
(35) Xu, G.-L.; Wang, C.-Y.; Ni, Y.-H.; Goodson, T. G., III; Ren, T. *Organometallics* **2005**, *24*, 3247–3254.
(36) Xu, G.-L.; Ren, T. *Organometallics* **2005**, *24*, 2564–2566.
(37) Xu, G.-L.; Crutchley, R. J.; DeRosa, M. C.; Pan, Q.-J.; Zhang, H.-X.; Wang, X.; Ren, T. *J. Am. Chem. Soc.* **2005**, *127*, 13354–13363.
(38) Szuchmacher Blum, A.; Ren, T.; Parish, D. A.; Trammell, S. A.; Moore, M. H.; Kushmerick, J. G.; Xu, G.-L.; Deschamps, J. R.; Pollack, S. K.; Shashidhar, R. *J. Am. Chem. Soc.* **2005**, *127*, 10010–10011.
(39) Arribas, G.; Barral, M. C.; Gonzalez-Prieto, R.; Jimenez-Aparicio, R.; Priego, J. L.; Torres, M. R.; Urbanos, F. A. *Inorg. Chem.* **2005**, *44*, 5770–5777.
(40) Barral, M. C.; Gonzalez-Prieto, R.; Jimenez-Aparicio, R.; Priego, J. L.; Royer, E. C.; Torres, M. R.; Urbanos, F. A. *Z. Anorg. Allg. Chem.* **2005**, *631*, 2075–2080.
(41) Mochizuki, K.; Kawamura, T.; Chang, H.-C.; Kitagawa, S. *Inorg. Chem.* **2006**, *45*, 3990–3997.
(42) Barral, M. C.; Gallo, T.; Herrero, S.; Jimenez-Aparicio, R.; Torres, M. R.; Urbanos, F. A. *Inorg. Chem.* **2006**, *45*, 3639–3647.
(43) Mikuriya, M.; Yoshioka, D.; Handa, M. *Coord. Chem. Rev.* **2006**, *250*, 2194–2211.
(44) Nakai, M.; Funabiki, T.; Ohtsuki, C.; Harada, M.; Ichimura, A.; Tanaka, R.; Kinoshita, I.; Mikuriya, M.; Benten, H.; Ohkita, H.; Ito, S.; Obata, M.; Yano, S. *Inorg. Chem.* **2006**, *45*, 3048–3056.
(45) Barral, M. C.; Gonzalez-Prieto, R.; Herrero, S.; Jimenez-Aparicio, R.; Priego, J. L.; Royer, E. C.; Torres, M. R.; Urbanos, F. A. *Polyhedron* **2004**, *23*, 2637–2644.
(46) Liao, Y.; Shum, W. W.; Miller, J. S. *J. Am. Chem. Soc.* **2002**, *124*, 9336–9337.
(47) Yoshioka, D.; Mikuriya, M.; Handa, M. *Chem. Lett.* **2002**, 1044–1045.
(48) Zhang, L.-Y.; Chen, J.-L.; Shi, L.-X.; Chen, Z.-N. *Organometallics* **2002**, *21*, 5919–5925.
(49) Lin, X. Q.; Kadish, K. M. *Anal. Chem.* **1985**, *57*, 1498–1501.
(50) Evans, D. F. *J. Chem. Soc.* **1959**, 2003–2005.

Table 1. Crystal Data, Data Collection, and Processing Parameters for $Ru_2(F_3ap)_4(NCS)$ **1** and $Ru_2(F_3ap)_3(F_2Oap)(NCS)$ **2**

	$Ru_2(F_3ap)_4(NCS)$ **1**	$Ru_2(F_3ap)_3(F_2Oap)(NCS)$ **2**
mol formula	$C_{48}H_{31}N_9F_{12}SRu_2$	$C_{45}H_{24}N_9OF_{11}SRu_2 \cdot 1/2CH_2Cl_2$
fw (g/mol)	1196.02	1192.40
space group	*P*4/*ncc* tetragonal	*C*2/*c* monoclinic
cell constant		
a (Å)	28.6662(5)	18.831(3)
b (Å)	28.6662(5)	11.499(2)
c (Å)	23.0963(8)	41.656(6)
α (deg)	90.00	90.00
β (deg)	90.00	101.234(3)
γ (deg)	90.00	90.00
V (Å^3)	18 979.4(8)	8848 (2)
Z	16	8
ρ_{calcd} (g/cm^3)	1.674	1.790
μ (mm^{-1})	0.774	0.886
λ (Mo Kα) (Å)	0.71073	0.71073
T (K)	223	223
R (F_o)[a]	0.0221	0.0522
R_w (F_o)[b]	0.0584	0.1272

[a] $R = \sum||F_o| - |F_c||/\sum|F_c|$. [b] $R_w = [\sum_w(|F_o| - |F_c|)^2/\sum_w|F_o|^2]^{1/2}$.

Synthesis of (3,1) $Ru_2(F_3ap)_4(NCS)$ 1. A mixture of (3,1) $Ru_2(F_3ap)_4Cl$ and NaSCN in a 1:4 molar ratio was stirred under inert atmosphere at room temperature in freshly distilled THF for 4 h. The solvent was then removed, and the crude product was extracted with diethyl ether and water (1:1, v/v). The organic layer was then concentrated and subjected to silica gel column chromatography using diethyl ether as eluent. Only a brown-green band was observed and collected to give a 70% yield. Mass spectral data [*m*/*e*, (fragment)]: 1153 $[Ru_2(F_3ap)_4(NCS)]^+$, 1093 $[Ru_2(F_3ap)_4]^+$. Anal. Calcd for $C_{48}H_{31}F_{12}N_9Ru_2S$: C, 48.20; H, 2.61; N, 10.54. Found: C, 47.97; H, 2.37; N, 10.49. UV–vis spectrum in CH_2Cl_2 [λ_{max}, nm ($\epsilon \times 10^{-3}$, M^{-1} cm^{-1})]: 434 (3.9) 482 (3.9) 781 (2.6). IR: $\nu_{SCN} = 2038$ cm^{-1}. Magnetic moment = 3.95 μ_B at room temperature.

Synthesis of (3,1) $Ru_2(F_3ap)_3(F_2Oap)(NCS)$ 2. A mixture of (3,1) $Ru_2(F_3ap)_4Cl$ and NaSCN in a 1:4 molar ratio was stirred for 18 h, at room temperature in THF solvent which had been left overnight after being distilled. The solvent was removed, and the crude product was subjected to silica gel column chromatography using diethyl ether as eluent. Two bands were observed and collected. Attempts to obtain crystals for X-ray diffraction were unsuccessful for the first fraction (brown greenish color), but the mass spectral data of this compound are consistent with the formulation $Ru_2(F_3ap)_4(NCS)$. The second band, which has a purple color, was the title compound as confirmed by the X-ray data. Yield: 30%. ^{1}HNMR (300 MHz, $CDCl_3$, 20 °C, *δ*): 9.3 (d, 1H), 9.0 (d, 1H), 8.8 (d, 2H), 8.3 (d, 2H), 7.7 (d, 2H), 7.4 (m, 3H), 7.1 (m, 1H), 6.9 (m, 2H), 6.6 (m, 8H), 6.3 (m, 2H). Mass spectral data [*m*/*e*, (fragment)]: 1149 $[Ru_2(F_3ap)_3(F_2Oap)(NCS)]^+$, 1091 $[Ru_2(F_3ap)_3(F_2Oap)]^+$. UV–vis spectrum in CH_2Cl_2 [λ_{max}, nm ($\epsilon \times 10^{-3}$, M^{-1} cm^{-1})]: 549 (3.3) 692 (sh) 865 (4.2) and 981 (sh). IR: $\nu_{SCN} = 2033$ cm^{-1}.

X-ray Crystallography. Crystals of **1** and **2** were each formed by slow diffusion of dichloromethane in hexane, and each crystal was analyzed as reported in the literature.[25] Final cell constants as well as other information pertinent to data collection and structure refinement are listed in Table 1. All measurements were made with a Siemens SMART platform diffractometer equipped with a 4K CCD APEX II detector for **1** and a 1K CCD area detector for **2**. All data for **1** and **2** were acquired following a procedure reported in the literature.[25] The Laue symmetry was determined to be 4/*mmm* for **1** and 2/*m* for **2** and from the systematic absences noted the space group was shown unambiguously to be *P*4/*ncc* tetragonal for **1** and *C*2/*c* monoclinic for **2**. Crystal data, data collection, and processing parameters for **1** and **2** are shown in Table 1.

The packing unit of **1** consists of a massive disordered solvent, hexanes, in pairs, surrounding a 222 site. Each location is further disordered into several different orientations. Only the two major orientations could be distinguished, comprising about 80% of the total occupancy, and these were refined using distance constraints for convenience. The crystal packing diagram clearly shows an empty 222 site where additional solvent should be located; however, because no significant electron density could be found it must be assumed that either this solvent was lost during sample preparation, or else the molecules are so excessively disordered that they are too weak to show up in different maps. The asymmetric unit of **2** consists of one Ru_2 molecule in a general position and $^1/_2$ molecule of methylene chloride solvent situated about a 2-fold axis. The solvent was found to be disordered over two slightly different orientations, and this was treated using ideal rigid body models, which were allowed to refine independently. A number of reflections having a poor fit between the observed and calculated structure factors had to be omitted as a result of excessive overlap of the diffraction peaks caused by the very long *c* axis.

Results and Discussion

Synthesis of (3,1) $Ru_2(F_3ap)_4(NCS)$ 1. The complex (3,1) $Ru_2(F_3ap)_4(NCS)$ was prepared by reacting (3,1) $Ru_2(F_3ap)_4Cl$ with excess NaSCN in freshly distilled THF for 4 h under a N_2 atmosphere according to eq 1.

$$(3,1)\ Ru_2(F_3ap)_4Cl + NaSCN \xrightarrow[r.t.,4h]{THF} (3,1)\ Ru_2(F_3ap)_4(NCS) + NaCl \quad (1)$$

Excess sodium thiocyanate was removed by extracting with water and the product was purified by column chromatography to give **1** in 70% yield. Only the monoisothiocyanato adduct was obtained even when the reaction time was extended to 18 h. A similar result was reported for the reaction between $Ru_2(O_2CMe)(DPhF)_3Cl$ and AgSCN,[45] where the axial SCN^- ligand substitutes for Cl^-. However, the room temperature magnetic moment of **1** is 3.95 μ_B (see Experimental Section), thus implying that **1** and its parent compound, $Ru_2(F_3ap)_4Cl$, both have three unpaired electrons. This result contrasts with what was reported upon conversion of $Ru_2(O_2CMe)(DPhF)_3Cl$ to $Ru_2(O_2CMe)(DPhF)_3(NCS)$, which is accompanied by a change from three to one unpaired electrons.[45] In this regard, it should be noted that the magnetic data obtained by Barral and co-workers[42,45] were obtained on compounds in the solid state, whereas magnetic measurements in the current study were made in solution. This may be the reason for the difference between the two results because magnetic properties of diruthenium complexes can be sensitive to small changes in the solid state[51,52] but these effects may be lost in solution.

Synthesis of $Ru_2(F_3ap)_3(F_2Oap)(NCS)$ 2. As described in the Experimental Section, the synthesis of **2** was carried

(51) Cotton, F. A.; Herrero, S.; Jimenez-Aparicio; Murillo, C. A.; Urbanos, F. A.; Villagran, D.; Wang, X. *J. Am. Chem. Soc.* **2007**, *129*, 12555–12667.

(52) Barral, M. C.; Gallo, T.; Herrero, S.; Jimenez-Aparicio, R.; Torres, M. R.; Urbanos, F. A. *Chem.—Eur. J.* **2007**, *13*, 10088–10095.

Table 2. Selected Bond Lengths (Angstroms) and Bond Angles (Degrees) for (3,1) $Ru_2(F_3ap)_4(NCS)$ **1** and (3,1) $Ru_2(F_3ap)_3(F_2Oap)(NCS)$ **2**

	$Ru_2(F_3ap)_4(NCS)$ **1**	$Ru_2(F_3ap)_3(F_2Oap)(NCS)$ **2**
	Bond Lengths (Angstroms)	
Ru−Ru	2.2830(3)	2.3328(8)
Ru−N	2.123(2)	2.231(6)
Ru−N_p[a]	2.091	2.083
Ru−N_a[a]	2.053	2.037
Ru−O		2.172(6)
	Bond Angles (Degrees)	
Ru−Ru−N	178.49(7)	175.99
Ru−N−C	176.5(2)	166.0
Ru−Ru−O		164.64(19)
Ru−O−C		110.6(5)
N−C−S	179.3(3)	179.1(7)
Ru−Ru−N_p[a]	88.9	90.7
Ru−Ru−N_a[a]	89.6	88.4
N_a−Ru−Ru−N_p[a]	17.0	4.9

[a] Average value. N_p: pyridyl nitrogen. N_a: anilino nitrogen.

out at room temperature for 18 h in THF left overnight after distillation. This synthesis is believed to occur via a radical mechanism with the origin of the inserted oxygen atom coming from peroxides, which were generated from oxygen and the utilized THF solvent as shown in eq 2. A similar mechanism was also proposed for the conversion of (3,1) $Ru_2(F_5ap)_4Cl$ to (3,1) $Ru_2(F_5ap)_3(F_4Oap)Cl$ when utilizing a THF solvent left overnight after distillation.[1,2] This mechanism is further confirmed by the fact that (3,1) $Ru_2(F_3ap)_4Cl$ is not converted to **2** when the reaction was carried out in freshly distilled THF nor does it occur in commercially available THF containing the known radical inhibitor 2,6-di-*tert*-butyl-4-methylphenol. However, it should be pointed out that the previously reported Ru_2^{6+} complex, (3,1) $Ru_2(F_5ap)_3(F_4Oap)Cl$, is paramagnetic,[53] whereas the newly synthesized Ru_2^{6+} complex is diamagnetic.

$$Ru_2(F_3ap)_4Cl + NaSCN \xrightarrow[\text{r.t., 18 h}]{\text{THF/peroxides}} Ru_2(F_3ap)_3(F_2Oap)(NCS) + NaCl \quad (2)$$

Molecular Structure. (3,1) $Ru_2(F_3ap)_4(NCS)$ **1** crystallizes in the tetragonal unit cell with space group *P4/ncc*, whereas (3,1) $Ru_2(F_3ap)(F_2Oap)(NCS)$ **2** crystallizes in the monoclinic unit cell with space group *C2/c*. Selected average bond lengths and average bond angles of **1** and **2** are listed in Table 2, whereas the ORTEP diagrams of the two compounds are shown respectively in parts a and b of Figure 1. In both complexes, the SCN^- axial ligand which replaces Cl^- from the parent compound is bound to the diruthenium core via its nitrogen. The Ru−Ru bond length increases upon going from **1** to **2** (2.2830 vs 2.3328 Å), but an opposite trend is observed for the averaged Ru−N_p and Ru−N_a bond distances (Table 2), which makes **2** more structurally compact than **1**. The Ru−Ru−N_{axial} and the N−C−S bond angles are similar for **1** and **2**, but the Ru−N−C bond angle of **1** is larger than the same bond angle of **2** (176.5 vs 166.0°). This latter difference is most likely due to a steric effect between the NCS group and the bridging ligand in **2** because the ν_{SCN} of

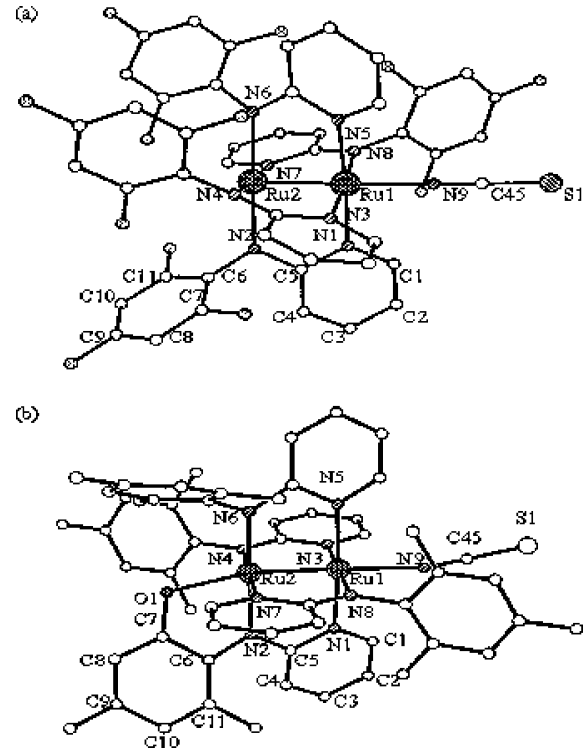

Figure 1. Molecular structures of (a) (3,1) $Ru_2(F_3ap)_4(NCS)$ **1** and (b) (3,1) $Ru_2(F_3ap)_3(F_2Oap)(NCS)$ **2**. Hydrogen atoms have been omitted for clarity.

1 (2038 cm^{-1}) and **2** (2033 cm^{-1}) do not differ significantly from each other.

The X-ray structure of **1** shows that the four F_3ap ligands occupy equatorial positions of the compound. The SCN anion is axially bound to one of the two ruthenium atoms via its nitrogen. As shown in part a of Figure 1, Ru1 is coordinated to three pyridyl nitrogen atoms, one anilino nitrogen atom, and one axial nitrogen atom, whereas Ru2 is coordinated to three anilino nitrogen atoms and one pyridyl nitrogen atom. Part a of Figure 1 shows that **1** retains the (3,1) isomeric conformation of its parent compound, $Ru_2(F_3ap)_4Cl$. No significant structural changes within the $Ru_2(L)_4$ framework are observed upon replacing Cl^- with SCN^-. Structural comparisons between **1** and $Ru_2(O_2CMe)(DPhF)_3(NCS)$[45] reveal that both compounds have similar N−C−S bond angles (178° vs 179°), but the Ru−NCS bond length of **1** (2.123 Å) is slightly longer than that of $Ru_2(O_2CMe)(DPhF)_3(NCS)$(2.103 Å).[45] The Ru−N−C bond angle of **1** (176.5°) is also much larger than that of $Ru_2(O_2CMe)(DPhF)_3(NCS)$[45] (167.7°). These structural differences might be accounted for by changes in the spin configuration of the two compounds because **1** has three unpaired electrons as opposed to one unpaired electron for $Ru_2(O_2CMe)(DPhF)_3(NCS)$, but differences in the type of bridging ligands cannot be ruled out as a factor because DPhF and O_2CMe are both symmetrical ligands, whereas F_3ap is unsymmetrical.

2 contains four bridging ligands, one of which is dianionic and is both axially and equatorially bound to one of the two ruthenium atoms as shown in part b of Figure 1. Each ruthenium ion in **2** exhibits a distorted octahedral coordina-

(53) Bear, J. L.; Li, Y.; Han, B.; Van Caemelbecke, E.; Kadish, K. M. *Inorg. Chem.* **1996**, *35*, 3053–5.

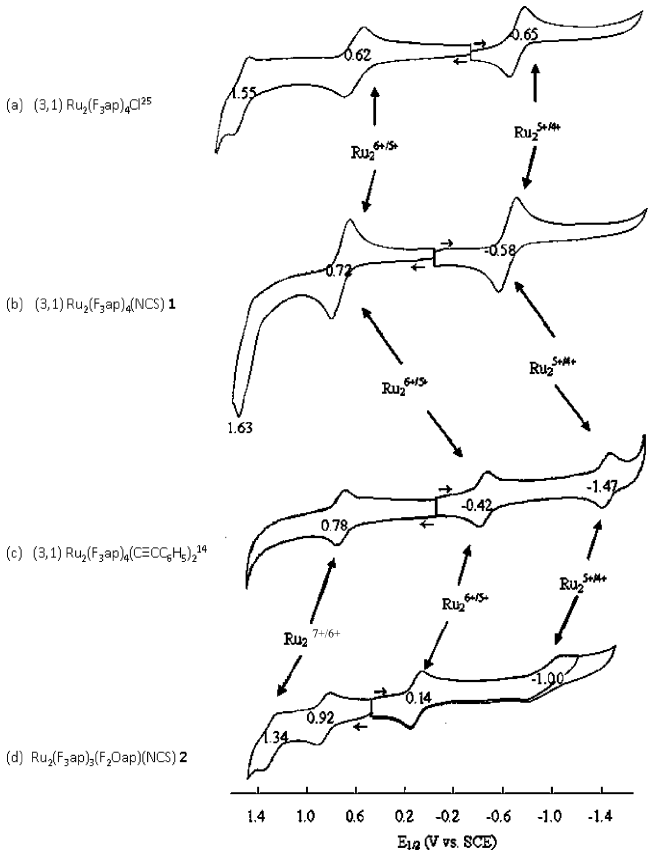

Figure 2. Cyclic voltammograms of (a) (3,1) $Ru_2(F_3ap)_4Cl$,[25] (b) (3,1) $Ru_2(F_3ap)_4(NCS)$ **1**, (c) (3,1) $Ru_2(F_3ap)_4(C'CC_6H_5)_2$,[14] and (d) (3,1) $Ru_2(F_3ap)_3(F_2Oap)(NCS)$ **2** in CH_2Cl_2, 0.1 M TBAP. Scan rate = 0.10 V/s.

tion, with four nitrogens forming the equatorial plane. Ru1 is coordinated to the nitrogen of the NCS axial ligand, three pyridyl nitrogen atoms, and one anilino nitrogen atom; whereas Ru2 is bound to an axial oxygen atom, three anilino nitrogen atoms, and one pyridyl nitrogen atom. The 2.3328(8) Å Ru−Ru bond length of **2** (Table 2) falls within the range of metal−metal bond lengths for other related compounds, namely (3,1) $Ru_2(F_5ap)_3(F_4Oap)Cl$ (2.336 Å),[1,53] (3,1) $Ru_2(F_5ap)_2(F_4Oap)(F_4NCNap)$ (2.332 Å),[1] and (3,1) $Ru_2(F_5ap)_2(F_4Oap)_2$ (2.308 Å).[1] The Ru−Ru bond length of **2**is also similar to the Ru−Ru bond lengths of other Ru_2^{6+} complexes with two axial ligands, examples being $Ru_2(hpp)_4Cl_2$ (2.321 Å),[32,53] $Ru_2(DMBA)_4Cl_2$ (2.323 Å),[28,32] and $Ru_2(DEBA)_4Cl_2$ (2.340 Å)[24,28] (hpp = 1,3,4,6,7,8-hexahydro-2H-pyrimido[1,2-a]pyrimidinate anion, DMBA = *N*,*N*′-dimethylbenzamidinate anion and DEBA = *N*,*N*′-diethylbenzamidinate anion. Finally, it should be pointed out that **2** and (3,1) $Ru_2(F_5ap)_3(F_4Oap)Cl$[51] have very similar bond lengths and bond angles, despite the fact that the former compound is diamagnetic and the latter is paramagnetic.

Electrochemistry. Figure 2 shows cyclic voltammograms of **1** and **2** in CH_2Cl_2 containing 0.1 M TBAP as well as (3,1) $Ru_2(F_3ap)_4Cl$ and (3,1) $Ru_2(F_3ap)_4(C\equiv CC_6H_5)_2$ under the same solution conditions for comparison purposes. Table 3 lists $E_{1/2}$ values for each redox reaction of the above four compounds. As shown in Figure 2 and Table 3, the substitution of Cl^- by SCN^- in $Ru_2(F_3ap)_4Cl$ to give **1** leads to a slight positive shift of all redox processes from the parent compound. The second oxidation of **1** also becomes irreversible and is located at $E_p = 1.63$ V for a scan rate of 0.10 V/s.

The structure of (3,1) $Ru_2(F_3ap)_3(F_2Oap)(NCS)$ **2** shows a Ru_2^{6+} complex with a quinone-type ligand on one of the two ruthenium atoms and a π-acceptor ligand on the other. Thus, one would expect to observe not only three redox processes associated with the addition or abstraction of electrons from the diruthenium unit but also a reaction associated with an easily oxidizable quinone-type ligand.[48] This indeed seems to be the case as shown by a comparison of the electrochemical data for the oxidation and reduction of $Ru_2(F_3ap)_4(C\equiv CC_6H_5)_2$ and **2** in CH_2Cl_2, 0.1 M TBAP (parts c and d of Figure 2). The electrochemistry of $Ru_2(F_3ap)_4(C\equiv CC_6H_5)_2$ has been reported in the literature[14] and is similar to that of related $Ru_2(L)_4(C\equiv CC_6H_5)_2$ derivatives (L = ap, Fap, or F_5ap), which contain a Ru_2^{6+} core in their neutral form.[14] As seen in part c of Figure 2, $Ru_2(F_3ap)_4(C\equiv CC_6H_5)_2$ undergoes two reversible reductions and one reversible oxidation at $E_{1/2} = -0.42$, -1.47, and 0.78 V vs SCE. Two reductions are also observed for **2** under the same solution conditions (part d of Figure 2). These occur at $E_{1/2} = +0.14$ and -1.00 V and are assigned to $Ru_2^{6+/5+}$ and $Ru_2^{5+/4+}$ processes, respectively. A similar assignment was earlier proposed for other Ru_2^{6+} complexes with a structure similar to **2**.[2] The difference in potential between the first one-electron reduction of $Ru_2(F_3ap)_4(C\equiv CC_6H_5)_2$ at -0.42 V (part c of Figure 2) and the first one-electron reduction of $Ru_2(F_3ap)_3(F_2Oap)(NCS)$ at 0.14 V (part d of Figure 2) is 560 mV with **2** being more easily reduced. A similar 560 mV shift in potential is also observed between the first one-electron oxidation of $Ru_2(F_3ap)_4(C\equiv CC_6H_5)_2$ at 0.78 V (part c of Figure 2) and the second one-electron oxidation of **2** at 1.34 V (part d of Figure 2). This later fact strongly suggests that the second oxidation of (3,1) $Ru_2(F_3ap)_3(F_2Oap)(NCS)$ is associated with the $Ru_2^{6+/7+}$ process of the compound, and the first oxidation at 0.92 V can then be assigned to a one-electron abstraction from the dianionic bridging ligand as was also reported in the case of the related compounds (3,1) $Ru_2(F_5ap)_3(F_4Oap)Cl$,[53] (3,1) $Ru_2(F_5ap)_2(F_4Oap)_2$[1] and (3,1) $Ru_2(F_5ap)_2(F_4Oap)(F_4NCNap)$[1] under the same experimental conditions. It should also be noted that the oxidation of hydroquinone in water occurs at 0.70 V,[54] and the positive shift of 0.22 V for the 0.92 V process in part d of Figure 2 may be accounted for by the strong electron-withdrawing effect of the trifluoroanilino ring.

As shown in Table 3, the electrochemical behavior of **2** resembles that of (3,1) $Ru_2(F_5ap)_3(F_4Oap)Cl$ despite the fact that the two Ru_2^{6+} complexes have a different number of unpaired electrons. Both compounds undergo two reductions and two oxidations, and shifts in $E_{1/2}$ values upon going from the electrode processes of (3,1) $Ru_2(F_5ap)_3(F_4Oap)Cl$ to those of **2** are attributed to changes in both equatorial and axial ligands.

UV–Vis Spectroscopy. Part a of Figure 3 shows the UV–vis spectrum of $Ru_2(F_3ap)_4(NCS)$ **1** in CH_2Cl_2 between

(54) Bailey, S. I.; Ritchie, I. M. *Electrochim. Acta* **1985**, 3–12.

Table 3. Half-Wave Potentials (V vs SCE) in CH_2Cl_2 Containing 0.1 M TBAP, Scan Rate = 0.10 V/s

		$E_{1/2}$ (V vs SCE)				
oxidative state	compound	other	reactions[b]	$Ru_2^{6+/5+}$	$Ru_2^{5+/4+}$	ref
Ru_2^{5+}	$Ru_2(F_3ap)_4Cl$		1.55	0.62	−0.65	25
	$Ru_2(F_3ap)_4(NCS)$ **1**		1.63[a]	0.72	−0.58	tw
Ru_2^{6+}	$Ru_2(F_3ap)_4(C_2C_6H_5)_2$		0.78	−0.42	−1.47	14
	$Ru_2(F_5ap)_3(F_4Oap)Cl$	1.35	0.98	0.22	−0.82	51
	$Ru_2(F_3ap)_3(F_2Oap)(NCS)$ **2**	1.34	0.9	0.14	−1.00	tw

[a] E_{pa} value at 0.10 V/s. tw: this work. [b] See text for details.

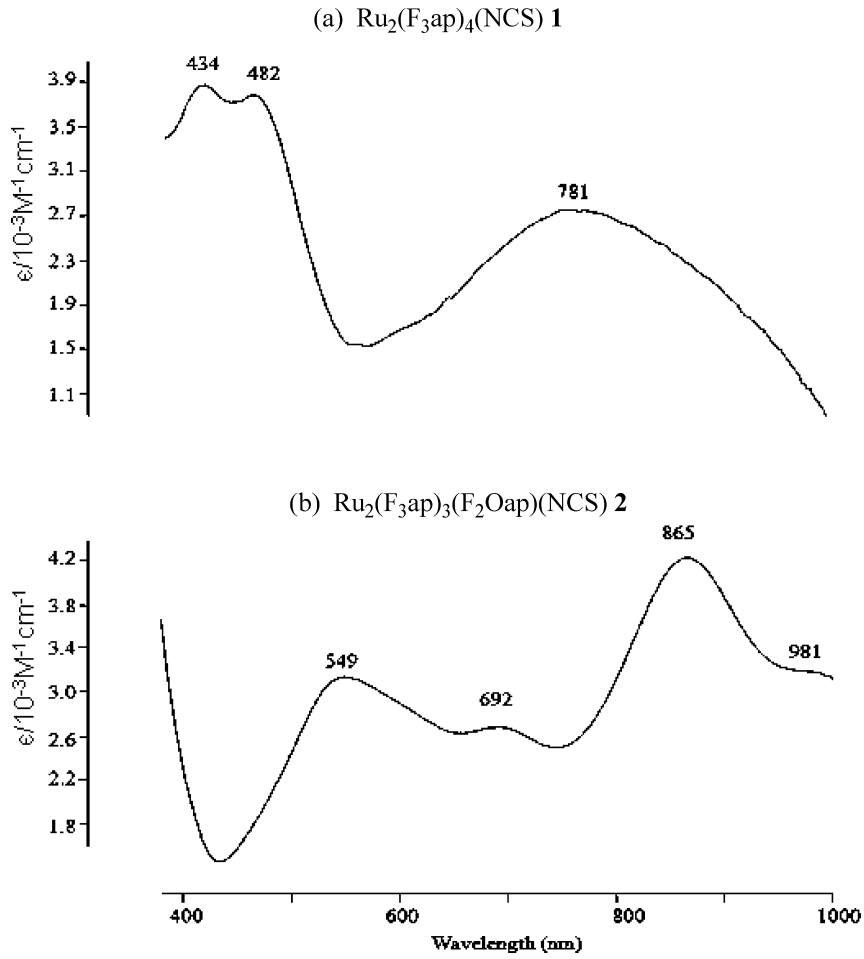

Figure 3. UV–Vis spectrum of (a) **1** and (b) **2** in CH_2Cl_2.

400 and 1000 nm. This spectrum has features that are typical of other (3,1) isomers of $Ru_2(F_xap)_4Cl$[25] (x = 1, 2, 3, or 5), with two high energy bands of similar wavelengths at 434 and 482 nm and one broad lower-energy band centered at 781 nm. The fact that the conversion of (3,1) $Ru_2(F_3ap)_4Cl$ to **1** is not accompanied by major spectral changes is consistent with the lack of change in the electronic configuration and what has been reported upon going from $Ru_2(O_2CMe)(DPhF)_3Cl$ to $Ru_2(O_2CMe)(DPhF)_3(NCS)$ where axial ligand exchange is accompanied by a change in the spin configuration.[42,45]

The UV–vis spectrum of $Ru_2(F_3ap)_3(F_2Oap)(NCS)$ **2** in CH_2Cl_2 is characterized by four absorption bands at 549, 692, 865, and 981 nm (part b of Figure 3) which can be compared to the four absorption bands of the (3,1) $Ru_2(F_5ap)_3(F_4Oap)Cl$ at 486, 623, 706, and 880 nm.[53] However, there is a clear difference in the spectral pattern in that all four bands of the latter compound have similar molar absorptivities, as opposed to bands with very different molar absorptivities in the case of **2**. These spectral differences might simply be accounted for by a change in the equatorial ligands (F_3ap vs F_5ap). However, as discussed in a later section of the manuscript, (3,1) $Ru_2(F_5ap)_3(F_4Oap)Cl$[53] and **2** also have different electronic configurations, which might also bring about spectral differences between the two compounds.

UV–Vis Spectroelectrochemistry. The UV–vis spectral changes which occur during the first oxidation and first reduction of $Ru_2(F_3ap)_4(NCS)$ **1** in CH_2Cl_2 containing 0.2 M TBAP, are shown in parts a and c of Figure 4. The oxidized form of **1** in part a of Figure 4 exhibits two major bands at 580 and 900 nm, which are reminiscent of the 487 and 965 nm bands seen in the Ru_2^{6+} form of $Ru_2(F_3ap)_4Cl$.[25] As shown in part c of Figure 4, the three absorption bands

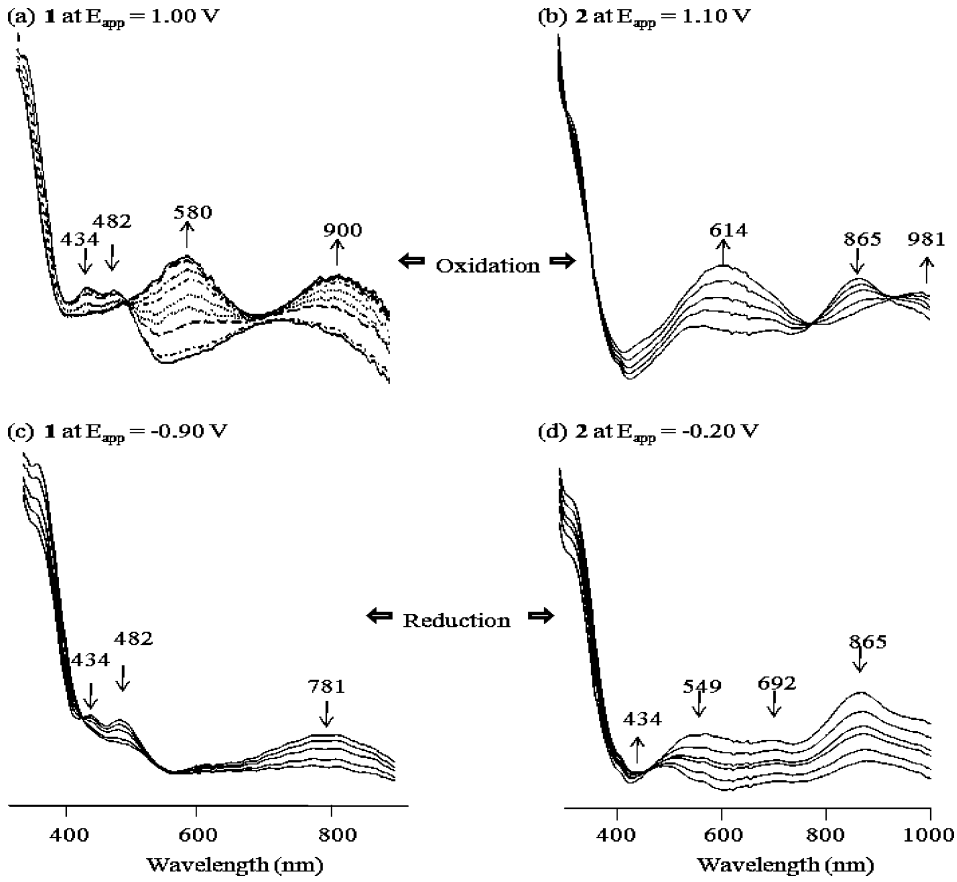

Figure 4. UV–vis spectral changes upon (a) oxidation of $Ru_2(F_3ap)_4(NCS)$ **1** at $E_{app} = 1.00$ V, (b) oxidation of $Ru_2(F_3ap)_3(F_2Oap)(NCS)$ **2** at $E_{app} = 1.10$ V, (c) reduction of $Ru_2(F_3ap)_4(NCS)$ **1** at $E_{app} = -0.90$ V, and (d) reduction of $Ru_2(F_3ap)_3(F_2Oap)(NCS)$ **2** at $E_{app} = -0.20$ V in CH_2Cl_2, 0.2 M TBAP.

at 434, 482, and 781 nm decrease in intensity during the $Ru_2^{5+} \rightarrow Ru_2^{4+}$ reaction, and the UV–vis spectrum after complete reduction of **1** displays a small absorption band at 510 nm. A very similar spectral pattern has been reported upon reduction of (3,1) $Ru_2(F_3ap)_4Cl$ in CH_2Cl_2, 0.2 M TBAP.[25] The reduction of the latter compound has been proposed to involve the addition of an electron to the π^* orbital, thus yielding a Ru_2^{4+} complex with the electronic configuration, $\sigma^2\pi^4\delta^2\pi^{*3}\delta^*$.[25] This electronic configuration is also proposed for the Ru_2^{4+} form of **1**.

Part b of Figure 4 illustrates the UV–vis spectral changes that occur upon the first one-electron oxidation of $Ru_2(F_3ap)_3(F_2Oap)(NCS)$ **2** in CH_2Cl_2, 0.2 M TBAP. As the oxidation proceeds at an applied potential of 1.10 V in the thin-layer cell, the band at 865 nm decreases in intensity, whereas two new bands appear at 614 and 981 nm. An isosbestic point is seen at 800 nm, thus suggesting that only the neutral and oxidized forms of the compound are in solution during the thin-layer electrolysis. These spectral changes are attributed to oxidation of the dianionic F_2Oap^{2-} ligand in **2**, consistent with the electrochemical data.

The UV–vis spectral changes upon reduction of **2** in CH_2Cl_2 containing 0.2 M TBAP at an applied potential of -0.20 V are illustrated in part d of Figure 4. There is a clear isosbestic point at 480 nm, and the reduced form of the compound is characterized by three absorption bands at 500, 692, and 867 nm. A UV–vis spectrum with three absorption bands at 492, 730, and 952 nm has also been reported for the Ru_2^{5+} form of $Ru_2(F_4Oap)(F_5ap)_3Cl$,[53] which suggests that the reduction of **2** is also a $Ru_2^{6+} \rightarrow Ru_2^{5+}$ process. This assignment agrees with the electrochemistry of the compound discussed earlier in the manuscript.

Electronic Configuration. 1 has a magnetic moment of 3.95 μ_B at room temperature, which implies that it has three unpaired electrons. Furthermore, **1** has structural, electrochemical, and spectroscopic properties similar to those of the parent compound, (3,1) $Ru_2(F_3ap)_4Cl$, thus implying that there is no change in the electronic configuration as SCN^- substitutes for Cl^- in (3,1) $Ru_2(F_3ap)_4Cl$. **2** is characterized by a well-defined ^1H NMR spectrum, which indicates that it has no unpaired electrons. Hence, **2** has neither the electronic configuration $\sigma^2\pi^4\delta^2(\pi^*\delta^*)^2$ nor $\sigma^2\pi^4\delta^2\pi^{*2}$, although these electronic configurations have been proposed for $Ru_2(F_5ap)_3(F_4Oap)Cl$, $Ru_2(F_5ap)_2(F_4Oap)_2$, and $Ru_2(F_5ap)_2(F_4Oap)(F_4NCNap)$,[1] all of which are Ru_2^{6+} complexes with a dianionic F_xOap^{2-} unit as in **2**. One other possible electronic structure for **2**, which would account for the absence of unpaired electrons, is $\pi^4\delta^2\pi^{*4}$ as has been proposed for (3,1) $Ru_2(F_3ap)_4(C{\equiv}CC_6H_5)_2$;[14] however, as pointed out earlier, the Ru−Ru bond length significantly decreases from 2.464 to 2.3328 Å upon going from (3,1) $Ru_2(F_3ap)_4(C{\equiv}CC_6H_5)_2$[14] to **2**, whereas the Ru−Ru bond length of **2** is similar to that of other Ru_2^{6+} complexes, which possess a quinone-type dianionic ligand. Therefore, the electronic configuration of $Ru_2(F_3ap)_3(F_2Oap)(NCS)$ **2** is most

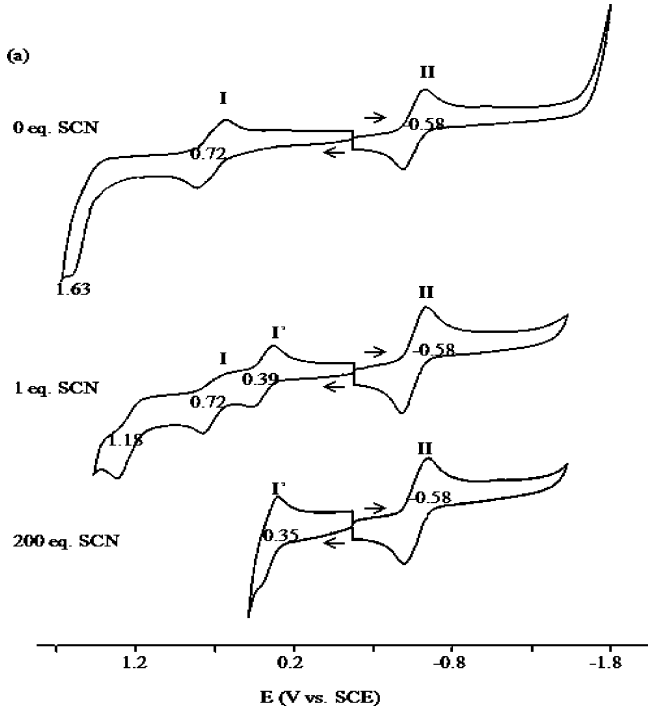

Figure 5. Cyclic voltammograms of 0.80 mM of (3,1) $Ru_2(F_3ap)_4(NCS)$ with 0, 1, and 200 eq TBASCN in CH_2Cl_2 containing 0.1 M TBAP.

likely $\sigma^2\pi^4\delta^2\delta^{*2}$due to the presence of the SCN^- axial ligand. It should be noted that a similar effect of the SCN group on the electronic structures has been reported for the two compounds, $Ru_2(O_2CMe)(DPhF)_3Cl$ and $Ru_2(O_2CMe)(DPhF)_3(NCS)$, the first of which has three unpaired electrons and the second one unpaired electron.[42,45]

Reactivity of (3,1) $Ru_2(F_3ap)_4(NCS)$ 1 with SCN^-. Figure 5 shows cyclic voltammograms of (3,1) $Ru_2(F_3ap)_4(NCS)$ **1** in CH_2Cl_2, 0.1 M TBAP, before and after TBASCN is added to solution. In the absence of added SCN^-, the $Ru_2^{5+/6+}$ process (process I) occurs at $E_{1/2} = 0.72$ V, whereas the $Ru_2^{5+/4+}$ reaction (process II) is located at -0.58 V (Figure 5). The addition of 1 eq of TBASCN to solution leads to no change in $E_{1/2}$ for the $Ru_2^{5+/4+}$ process, but a new oxidation appears at a potential prior to process I and is labeled as I′ in Figure 5. The anodic peak currents for processes I and I′ are similar under these solution conditions, and the sum of the peak currents for the two oxidations are approximately equal to that for the reduction process II (Figure 5), thus suggesting that I and I′ can both be attributed to the oxidation of **1** with different final products after the electron abstraction.

It is proposed that process I yields the mono-NCS adduct $[Ru_2(F_3ap)_4(NCS)]^+$ at $E_{1/2} = 0.72$ V, whereas process I′ gives the bis-NCS adduct $Ru_2(F_3ap)_4(NCS)_2$ after the addition of a second SCN^- axial ligand, and this shifts the $E_{1/2}$ to 0.39 V in CH_2Cl_2 containing 1.0 eq of added SCN^-.

Further evidence for the above proposed mechanism is given by a plot of $E_{1/2}$ versus log[SCN^-] for processes I′ and II. This plot is shown in Figure 6 and can be divided into two regions labeled as A and B. The $E_{1/2}$ for the first oxidation in region A is linearly related to log[SCN^-] with a slope of -61 mV. This can be interpreted by a reaction

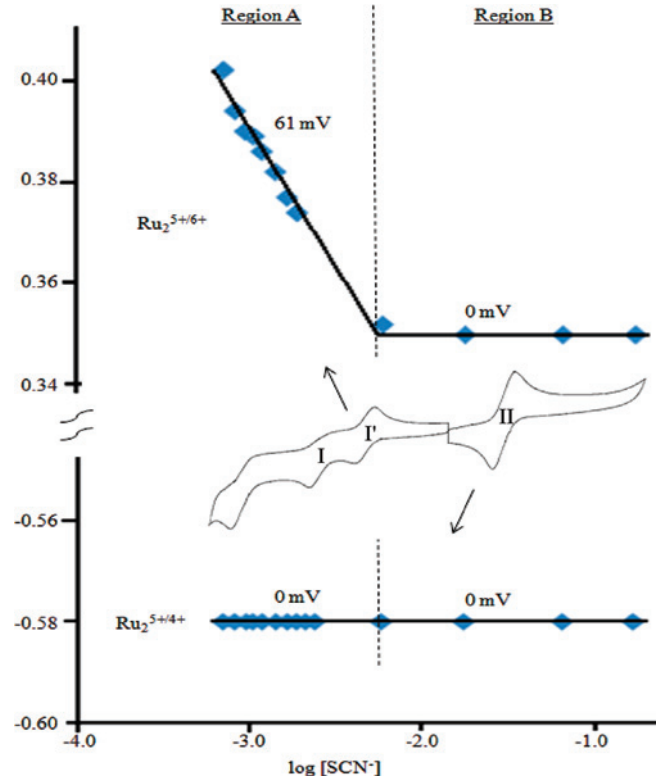

Figure 6. Plot of $E_{1/2}$ vs log [SCN^-] for the peak labeled I′ and II in Figure 5.

Scheme 1

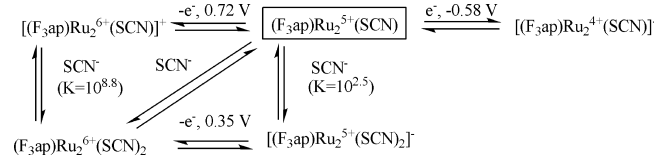

where **1** binds a single SCN^- anion upon oxidation to Ru_2^{6+}, giving $Ru_2(F_3ap)_4(NCS)_2$ as a final product. The $E_{1/2}$ for process I′ does not change with log[SCN^-] in region B of Figure 6, thus indicating that within this range of SCN^- concentration, the prevailing redox reaction is $[Ru_2(F_3ap)_4(NCS)_2]^-$ to $Ru_2(F_3ap)_4(NCS)_2$ as also shown in Scheme 1.

The formation constant for binding of a second SCN^- axial ligand to the Ru_2^{6+} form of (3,1) $Ru_2(F_3ap)_4(NCS)$ is calculated as $10^{8.8}$ using eq 3, which relates the potentials of the complexed and uncomplexed compounds to the concentration of free SCN^- in solution.[55] A stability constant for the conversion of $Ru_2(F_3ap)_4(NCS)$ to $[Ru_2(F_3ap)_4(NCS)_2]^-$ was computed as $10^{2.5}$ by combining the data in Figures 5, 6, and eq 3 and indicates a weak binding affinity for the addition of a second SCN^- axial ligand to the Ru_2^{5+} form of the compound.

$$E_{1/2}{}^{ML} = E_{1/2}{}^{M} - \frac{0.059}{n}\log K^{ML} - \frac{0.059}{n}\log[L]^p \quad (3)$$

Finally, it should be pointed out that $E_{1/2}$ for the $Ru_2^{5+/4+}$ reduction process (labeled as II in Figure 6) remained unchanged at all concentrations of SCN^- between 10^{-3} and

(55) Lingane, J. J. *Chem. Rev.* **1941**, 1–35.

10^{-1} M. This is shown in Figure 6, where $E_{1/2}$ is independent of log[SCN^-]. Thus, upon reduction, one SCN^- most likely dissociates from $[Ru_2(F_3ap)_4(NCS)_2]^-$ prior to electron addition. The overall mechanism for the one-electron reduction and one-electron oxidation of **1** in CH_2Cl_2, 0.1 M TBAP containing added SCN^- is described in Scheme 1. Not shown in the scheme is an additional oxidation, which occurs in the presence of 1 equiv SCN^- (Figure 5). This reaction is located at $E_{1/2} = 1.18$ V and is assigned to the $Ru_2^{6+/7+}$ process of $Ru_2(F_3ap)_4(NCS)_2$.

In summary, we have characterized redox properties of three different diruthenium compounds with one or two SCN^- axial ligands. The $Ru_2^{5+/6+}$ process varies from 0.14 V in the case of $Ru_2(F_3ap)_3(F_2Oap)(NCS)$ **2** to 0.72 V in the case of $Ru_2(F_3ap)_4(NCS)$ **1**. Of some significance is that the latter reaction can be shifted to 0.35 V in the presence of excess SCN^- where the prevailing redox couple is $[Ru_2(F_3ap)_4(NCS)_2]^-/Ru_2(F_3ap)_4(NCS)_2$. This is one of the easiest Ru_2^{5+} oxidations of any diruthenium (III, II) complex with a Ru_2L_4 structure and suggests that the type of anionic axial ligand is as important a factor in controlling redox properties of the compound as is the nature of the four bridging ligands.

Acknowledgment. Authors from the University of Houston are grateful for support from the Robert A. Welch Foundation (J.L.B., Grant E-918; K.M.K., Grant E-680). TSU authors thank the TSU Seed Grant-RCMI. We also thank Dr. J. D. Korp for X-ray analyses.

Supporting Information Available: X-ray crystallographic files, in CIF format, for **1** and **2**. This material is available free of charge via the Internet at http://pubs.acs.org.

IC8000703